BIOCHEMISTRY
including biophysical chemistry & molecular biology

Article

pubs.acs.org/biochemistry

^{19}F NMR Studies of a Desolvated Near-Native Protein Folding Intermediate

Julianne L. Kitevski-LeBlanc,[†,§] Joshua Hoang,[†,§] William Thach,[‡] Sacha Thierry Larda,[†] and R. Scott Prosser*[,†,‡]

[†]Department of Chemistry, University of Toronto, UTM, 3359 Mississauga Road North, Mississauga, Ontario L5L 1C6, Canada
[‡]Department of Biochemistry, University of Toronto, 1 King's College Circle, Toronto, Ontario M5S 1A8, Canada

Supporting Information

ABSTRACT: Although many proteins are recognized to undergo folding via an intermediate, the microscopic nature of folding intermediates is less understood. In this study, ^{19}F NMR and near-UV circular dichroism (CD) are used to characterize a transition to a thermal folding intermediate of calmodulin, a water-soluble protein, which is biosynthetically enriched with 3-fluorophenylalanine (3F-Phe). ^{19}F NMR solvent isotope shifts, resulting from replacing H_2O with D_2O, and paramagnetic shifts arising from dissolved O_2 are used to monitor changes in the water accessibility and hydrophobicity of the protein interior as the protein progresses from a native state to an unfolded state along a heat-denaturation pathway. In comparison to the native state, the solvent isotope shifts reveal the decreased presence of water in the hydrophobic core, whereas the paramagnetic shifts show the increased hydrophobicity of this folding intermediate. ^{15}N,^{1}H and methyl ^{13}C,^{1}H HSQC NMR spectra demonstrate that this folding intermediate retains a near-native tertiary structure whose hydrophobic interior is highly dynamic. ^{19}F NMR CPMG relaxation dispersion measurements suggest the near-native state is transiently adopted well below the temperature associated with its onset.

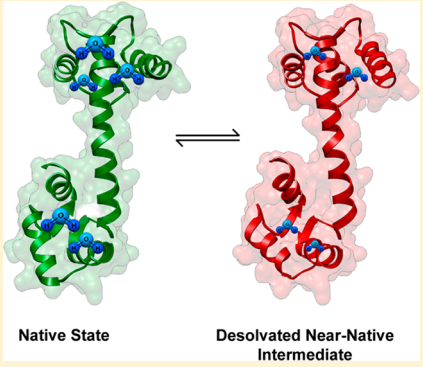

Despite the astronomical number of possible conformations available to polypeptides, folding is remarkably fast.[1] Proteins accomplish this feat in part because of early nucleation events in which secondary structure and main-chain hydrogen bonds are rapidly established, thereby guiding the search toward a compact folded state.[2−7] In some cases, an intermediate state is acquired where the ensemble of conformers are generally described as being near-native in structure. Although the intermediate state is believed to be highly dynamic, there remains a controversy as to the role of water in the intermediate. Many globular proteins have been shown to adopt intermediate states that are molten-globule-like. Their conformations, which are expanded and highly hydrated, retain native-like secondary structure yet lack significant tertiary structure.[8−10] The folding intermediate then undergoes hydrophobic collapse to give rise to the final folded state.[5−7] However, in other cases, the folding intermediate is believed to adopt a dry molten-globule state whose interior is best characterized as largely desolvated, liquid alkanelike, and stabilized by configurational entropy.[11,12] In this case, the final folding step is characterized by the restriction of side chains and increased van der Waals interactions. The existence of such a dry near-native folding intermediate poses several fundamental questions. For example, to what extent might such dry near-native intermediate states serve a functional role, allowing proteins to access biologically important excited states or, indeed, irreversibly misfolded states?

In this study, we explore the hierarchy of events involved in the reversible folding of a ubiquitous calcium-binding protein, calmodulin (CaM), using temperature to perturb the native state. Higher temperatures bring about a folding intermediate, consistent with previous descriptions of a dry molten-globule state in which the protein interior is dynamic yet desolvated. Even at temperatures near physiological conditions, the protein is observed to undergo millisecond time scale excursions to this intermediate state. Using ^{19}F NMR, we examine the properties of the protein interior, namely, solvent exposure and hydrophobicity, that are associated with the dry near-native state. ^{19}F NMR is uniquely sensitive to changes in conformation and environment (specifically, solvent exposure and hydrophobicity).

CaM is composed of two structurally analogous N- and C-terminal domains separated by a flexible helical linker, which facilitates the binding to its intended protein targets.[13] The X-ray crystal structure of calcium-loaded CaM depicts a dumbbell arrangement (Figure 1a). NMR studies have shown that the solution-state structure is far more dynamic than that represented by the crystal structure, where the helical linker allows the two domains to reorient almost independently of each other.[14,15] Despite the rich ensemble of conformations available to CaM, it is remarkably robust with regard to thermal denaturation; typical differential scanning calorimetry (DSC)

Received: July 25, 2013
Published: August 1, 2013

   dx.doi.org/10.1021/bi4010057 | *Biochemistry* 2013, 52, 5780−5789

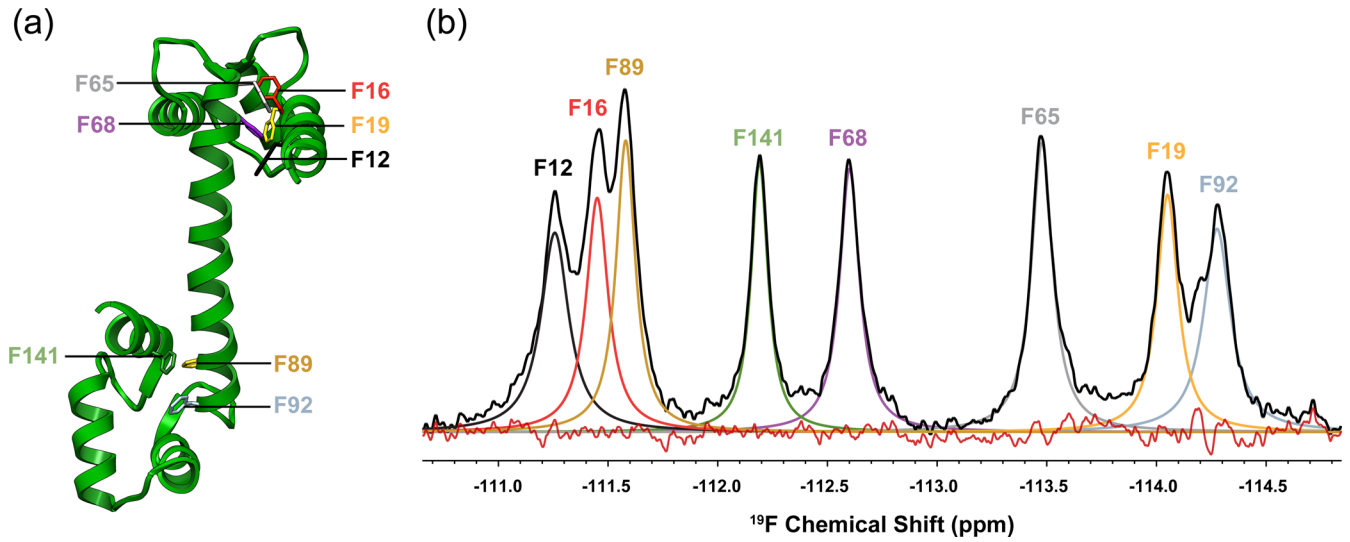

Figure 1. X-ray crystal structure and ^{19}F NMR spectrum of CaM. (a) X-ray crystal structure of the calcium-loaded state of CaM, highlighting the location of each phenylalanine residue (PDB file 3CLN). (b) ^{19}F NMR spectrum, collected at 50 °C, of 70% 3F-Phe fractionally labeled CaM. A spectral deconvolution is shown to distinguish all eight 3F-Phe resonances.

melt curves exhibit a broad transition around 115 °C.[16] Recent single-molecule force microscopy studies suggest that CaM exhibits a complex folding process, involving both on- and off-pathway folding intermediates.[17,18] However, a detailed microscopic description of the nature of the folding intermediates is still missing, as is a description of the potentially faster folding steps.

^{19}F NMR provides the means to study the hydrophobic interior without introducing gross changes to the protein. The ^{19}F nucleus is a sensitive NMR probe of the environment and hence protein topology through both chemical shifts and spin relaxation (T_1 and T_2).[19,20] Fluoroaromatics in particular exhibit a significant range of relaxation rates and chemical-shielding effects that depend sensitively on topology.[21] Thus, unfolding events would be expected to give rise to sizable chemical-shift effects for fluoroaromatics located in the protein's hydrophobic interior. This is advantageous because it allows for the sampling and characterization of transient states that may be difficult to detect by traditional ^{13}C,^{1}H and ^{15}N,^{1}H HSQC spectra.

The roles of water and hydrophobicity are of considerable importance in the folding process. Water is difficult to study by ^{1}H NMR through NOESY and ROESY experiments because of exchange-relayed artifacts from rapidly exchanging protons.[22] This has been recently addressed and could in principle be used to study water accessibility in CaM.[23] A variety of other approaches have been introduced to assess water encounters and exchange rates.[10,22,24−29] Here, however, we make use of ^{19}F NMR solvent isotope shifts, which provide a direct measure of the average accessibility in the protein interior without the need for bulky probes. We further demonstrate an approach to site-specifically measure hydrophobicity in the protein interior, which we interpret in terms of the folding process. Monofluorinated aromatics, such as 3-fluorophenylalanine (3F-Phe) used in this study, can be easily incorporated into CaM by biosynthetic means and generally give rise to few structural or functional perturbations.[30] All eight 3F-Phe residues can be resolved in the ^{19}F NMR spectrum of the native state of 3F-Phe-enriched CaM (Figure 1b). We present both circular dichroism (CD) and ^{19}F NMR evidence of a folding intermediate, which can be characterized as a dry near-native state.[11,12,31]

EXPERIMENTAL PROCEDURES

Protein Expression and Purification. The expression and purification of uniformly ^{15}N-enriched, 3F-Phe fractionally labeled CaM was performed as described previously with small modifications (Supporting Information).[30]

Circular Dichroism Spectroscopy. CD spectra in the far-UV (200−250 nm) and near-UV (253−273 nm) regions were acquired on an Aviv CD spectrometer model 62DS. Spectra of 5 mg/mL of 70% fractionally labeled 3-FPhe CaM, in 0.1 M KCl, 20 mM Tris HCl, and 9 mM $CaCl_2$ buffer adjusted to pH 8, were collected from 20 to 100 °C (in 5 °C increments) (path length, 0.1 cm; steps, 0.05 nm; bandwidth, 1 nm; and averaging time, 0.2 s).

NMR Experiments. NMR experiments were performed on a 500 MHz Varian Inova (^{1}H,^{1}H NOESY measurements and ^{15}N,^{1}H-detected aliphatic saturation spin diffusion), 600 MHz Varian Inova spectrometer (^{19}F NMR solvent isotope shifts, ^{19}F NMR O_2 shift experiments, ^{1}H stimulated echo diffusion NMR, ^{15}N,^{1}H spectroscopy, and ^{19}F NMR CPMG studies), and a 700 MHz Agilent spectrometer (^{13}C,^{1}H SOFAST HMQC spectra) (Agilent Technologies, Santa Clara, CA) using a combination of room temperature and cryogenic single gradient solution NMR probe tunable to either ^{1}H or ^{19}F on the high-frequency channel.

Further details of NMR experiments performed at the different field strengths are provided in the Supporting Information. All NMR data was processed using either the NMRPipe[32] or Mestrenova software.

Solvent Isotope Shifts. Solvent isotope shifts were evaluated by increasing the D_2O/H_2O fraction of the CaM sample from 10 to 100%. ^{19}F 1D spectra of ∼1.5 mM CaM in both solvents were obtained as a function of the temperature.

O_2 Paramagnetic Shifts. Paramagnetic shifts from dissolved oxygen were obtained by equilibrating the protein sample at a partial pressure of 10−25 atm overnight in a 5 mm o.d. and 3 mm i.d. sapphire NMR sample tube (Saint-Gobain Saphikon Crystals, Milford, NH, USA). The pressure during

dx.doi.org/10.1021/bi4010057 | Biochemistry 2013, 52, 5780−5789

the entire course of the NMR experiment was kept constant through the use of Swagelok (Swagelok, Solon, OH, USA) connections to a pressurized oxygen supply. ^{19}F 1D spectra of ~1.5 mM CaM, in both the absence and presence of dissolved oxygen, were obtained as a function of the temperature.

RESULTS

CD and ^{19}F NMR Evidence of a Folding Intermediate along a Heat-Denaturation Pathway. Although folding events under nondenaturing conditions often occur on a microsecond time scale and are thus difficult to capture by NMR, it is possible to spectroscopically discriminate a hierarchy of events along a temperature-denaturation pathway, as suggested in Figure 2. Of course, one must be cautious about making conclusions regarding temporal folding on the basis of heat or urea denaturation given the likelihood that heat or urea dramatically change the folding-energy landscape. In this study, we identify an intermediate by both heat denaturation and at lower temperatures by CPMG relaxation dispersion measurements, as discussed below. To begin, the far-UV CD and ^{15}N,^{1}H NMR spectra of CaM reveal that the secondary structure is largely retained over the entire range of temperatures studied (25−75 °C). The far-UV CD traces all exhibit the characteristic double minima, representative of α-helical structure, although the ellipticity decreases slightly at higher temperatures (Supporting Information, Figure S1a). ^{15}N,^{1}H spectra of the protein backbone largely tell the same story; the chemical-shift dispersion is consistent with a single state whose secondary structure and overall topology is very near that of the native state (Figure 3a). However, the near-UV CD behavior tends to be sensitive to the tertiary structure and compactness. Because CaM contains only two tyrosine residues and no tryptophan residues, the near-UV CD signature from 253 to 275 nm (Supporting Information, Figure S1b) largely reflects the packing environment in the vicinity of the phenylalanines. As the approximate CD profile is also reproduced at all temperatures, we consider the average ellipticity in this wavelength regime, $\langle\theta\rangle_{253-275}$, and plot this as a function of temperature (Figure 2). Generally, the average ellipticity gradually increases (toward 0) with increased temperature until 60 °C, pointing to an overall loss of tertiary structure and compactness of the hydrophobic core. Between 60 and 75 °C, the ellipticity is represented by a plateau, which we associate with a folding intermediate. Above this regime, ellipticity again increases with temperature, signifying a further loss of structure and compactness; a very similar result is observed with nonfluorinated CaM. It is also insightful to consider the ratio of near-UV to far-UV CD ($\langle\theta\rangle_{253-275}/\theta_{222}$), which exhibits a prominent discontinuity between 60 and 70 °C (Supporting Information, Figure S1c). On the basis of the far-

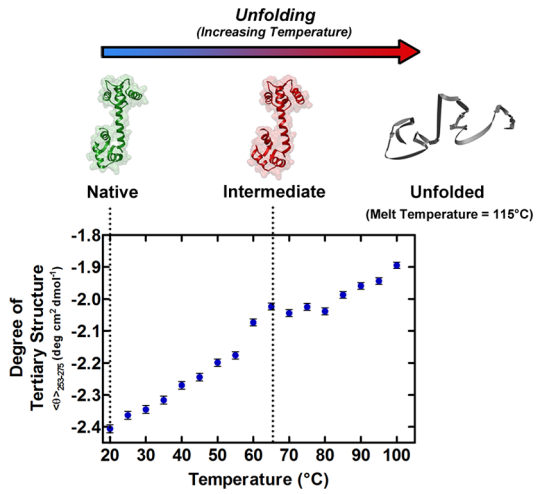

Figure 2. Changes in the degree of the tertiary structure of 3F-Phe CaM as a function of temperature, as monitored by the near-UV ellipticity signature, $\langle\theta\rangle_{253-275}$. As highlighted, a plateau in the degree of the tertiary structure seen from 65 to 80 °C signifies the onset of an intermediate state. At higher temperatures, beyond 80 °C, the protein gradually acquires a more unfolded state.

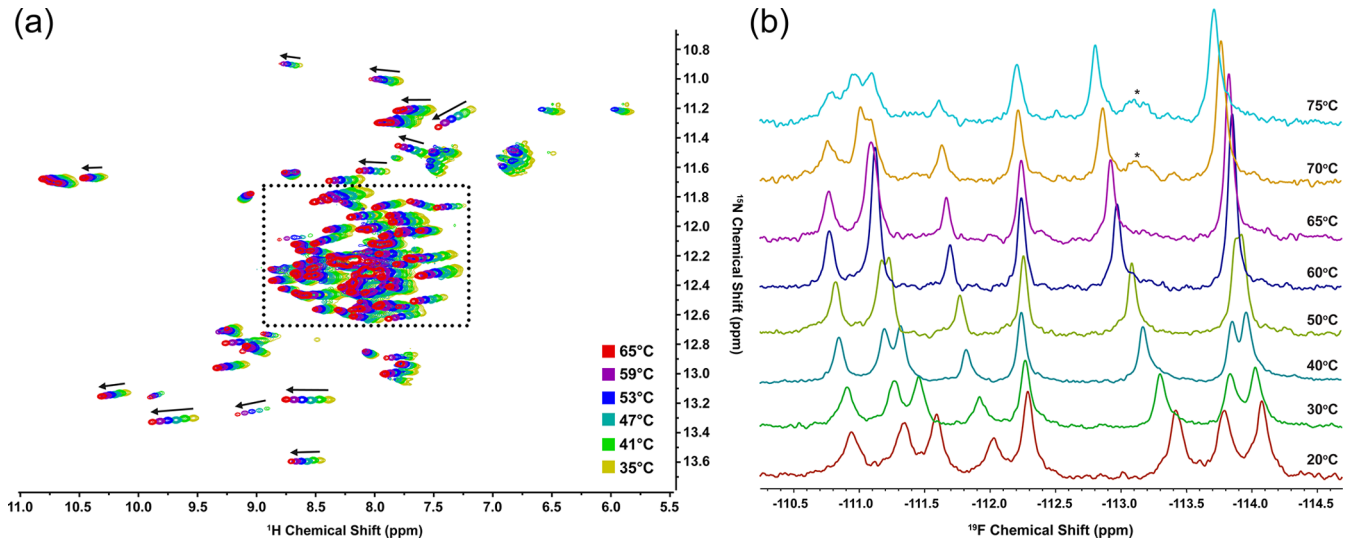

Figure 3. ^{15}N,^{1}H HSQC and ^{19}F NMR spectra (panels a and b, respectively) of 70% 3F-Phe fractionally labeled CaM as a function of temperature. Note that the boxed region is expanded in Figure S2. The chemical-shift dispersion and line widths in the HSQC spectra are consistent with a single folded state over the temperature range examined. However, the ^{19}F NMR spectra exhibit the onset of line broadening and hence an exchange process above 50 °C. Above 70 °C, very weak and broad ^{19}F resonances arise, between −113.3 and −113.7 ppm, as shown above by the peaks denoted with an asterisk. This may reflect the onset of an unfolded or aggregated state.

dx.doi.org/10.1021/bi4010057 | Biochemistry 2013, 52, 5780−5789

UV CD and ^{15}N,^{1}H spectra, this folding intermediate is best represented by a near-native conformation.

Although near-UV CD gives a hint of a folding intermediate, ^{19}F NMR provides a wealth of data regarding the equilibrium of folding states and their microscopic properties. As shown by the ^{19}F spectra (Figure 3b), a single Lorentzian line is observed for each 3F-Phe labeled site at any one temperature, signifying either a single state at low temperatures or fast exchange between a native and near-native states at higher temperatures (~40−70 °C). The existence of a single Lorentzian, arising from each 3F-Phe species, also signifies rapid ring flipping (on a chemical-shift scale), as has been noted previously,[33−35] and underlies the extent of the side-chain dynamics inherent in the hydrophobic protein interior. At 70 °C and higher, we begin to see the formation of additional minor peaks, which we associate with the onset of either an unfolded or an aggregated state. The temperature dependence of the chemical shifts of the dominant peaks is again consistent with a folding intermediate at 66 °C on the basis of a prominent nonlinear dependence of the chemical shift with temperature (Figure 4a). Although all eight resonances exhibit, to some degree, a nonlinear dependence of shift with temperature, four resonances, originating from residues 12, 16, 19, and 92, were found to exhibit a significant nonlinear dependence, which were sufficient to reliably extract the relative populations and estimates for a transition temperature, T_{NI}, and a transition width, Δ (Supporting Information, Figure S3). In this analysis (Supporting Information), we assume that in the temperature range of interest (25−70 °C) the protein is represented by a native state whose population is given by $p_1(T)$ and by a near-native intermediate whose population is given by $p_2(T)$, where $p_1(T) + p_2(T) = 1$. We further assume that both the native states and near-native states alone are characterized by a linear dependence of chemical shift with temperature. The final analysis produces a consistent description of the transition temperature, T_{NI} (66 ± 15 °C), and transition width, Δ (10 ± 7 °C). On the basis solely of the ^{19}F NMR chemical shifts, the transition to the near-native intermediate does not appear to be highly cooperative. However, the near-UV CD, ^{19}F NMR shifts, ^{19}F NMR solvent isotope shifts, and O_2-induced paramagnetic shifts (vide infra) all point to a common transition at 66 ± 5 °C. Figure 4b provides a graphical illustration of the estimates for the relative fraction of the near-native intermediate state as a function of temperature on the basis of the fitted values of T_{NI} and Δ for each ^{19}F resonance.

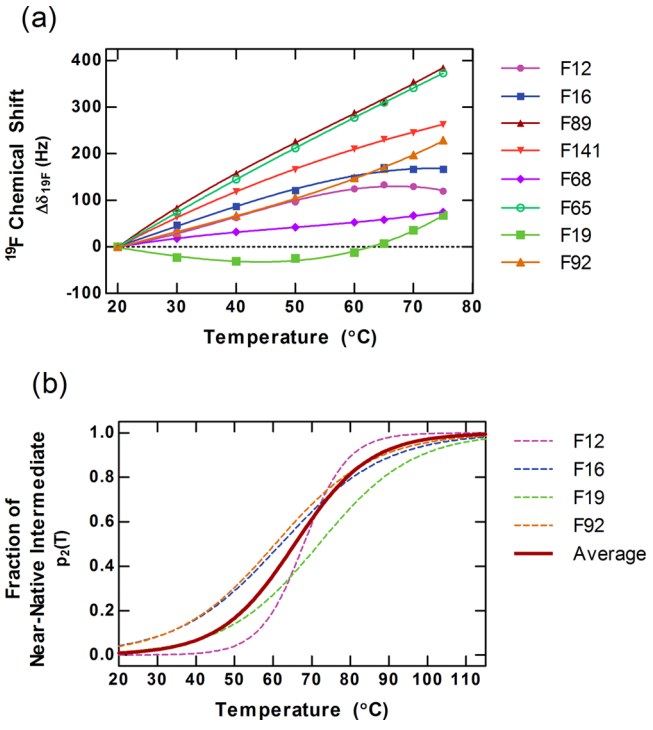

Figure 4. Population of the near-native intermediate derived from ^{19}F chemical-shift changes. (a) Temperature-dependent plot of the change in the ^{19}F chemical shift ($\Delta\delta_{19F}$), relative to the shift at 20 °C, associated with each of the eight 3F-Phe residues. Each fit was obtained using eqs 1 and 2 in the Supporting Information, from which the fitting parameters (T_{NI} and Δ) could be estimated. (b) Estimates of the temperature dependence of the relative fraction of the near-native intermediate state, $p_2(T)$, on the basis of the individual fits of shift versus temperature for residues 12 (purple), 16 (blue), 19 (green), and 92 (orange). $p_2(T)$ is parametrized exclusively by the transition temperature and width (T_{NI} and Δ). An average transition temperature (66 ± 15 °C) and width (10 ± 7 °C) is also estimated, and the resulting profile for $p_2(T)$ is represented by a solid line (red).

Solvent Exposure and Hydrophobicity along the Temperature-Denaturation Pathway. The presence of water is conveniently detected by ^{19}F NMR through the solvent isotope shift (i.e., the change in the chemical shift, introduced by replacing H_2O with D_2O). Moreover, the magnitude of the solvent isotope shift can be quantitatively related to the extent of solvent exposure.[36,37] We define a normalized solvent isotope shift, $\Delta\delta^*(H_2O)$, in which the relative difference between the chemical shifts in D_2O and H_2O at a site of interest is divided by the corresponding shift difference from an internal standard, 4F-Phe, added to the protein solution.

Figure 5 reveals the normalized solvent isotope shifts as a function of temperature. At 30 °C, solvent isotope shifts of the majority of fluorophenylalanine probes range between 25 and 55% of the fully exposed standard, suggesting the significant accessibility of water. In particular, the solvent isotope shifts associated with Phe-89 and Phe-92 are 45−55% of that of the fully exposed standard at 30 °C. Although these residues are buried in the apo structure,[38] the X-ray crystal structures reveal that Phe-89 and Phe-92 become significantly more solvent exposed upon the binding of the protein to calcium ions.[39] However, in general, we observe no apparent correlation between the measured solvent isotope shifts and the solvent

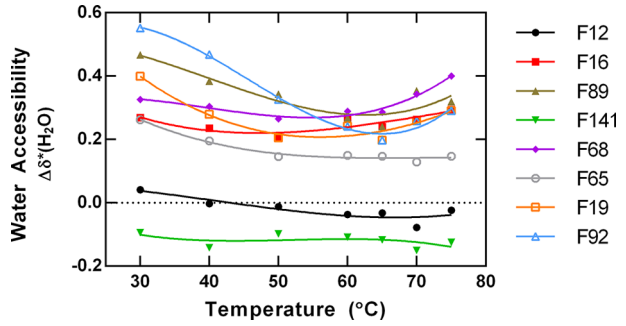

Figure 5. Temperature dependence of the ^{19}F solvent isotope shifts, $\Delta\delta^*(H_2O)$. The solvent isotope shifts are normalized by an internal standard, 4F-Phe, and provide a quantitative measure of solvent accessibility.

dx.doi.org/10.1021/bi4010057 | Biochemistry 2013, 52, 5780−5789

exposed surface area predicted by the X-ray crystal structure. We attribute this to the fact that X-ray crystal structures do not adequately account for the dynamic nature of proteins.[40] In particular, single-molecule force spectroscopy experiments reveal a complex landscape consisting of both the native state and higher-energy states, some of which are likely more solvent exposed.[17] Thus, in our case, we expect that both water and O_2 (discussed below) diffusively encounter the protein interior via a vast ensemble of rapidly interconverting conformers, including the most highly populated ground-state X-ray structure.[41] Note that although solvent isotope shifts are typically positive as defined, two residues exhibit negative solvent isotope shifts. The negative shifts are likely due to slight conformational perturbations resulting from the substitution of H_2O for D_2O. In general, D_2O tends to reinforce hydrogen bonds within alpha helices while minimally perturbing protein structure. Nevertheless, the solvent isotope shifts clearly indicate decreased solvent exposure with temperature, up to approximately 65 °C. Therefore, we conclude that in the native state water is gradually expelled from the hydrophobic core, driven at least in part by the relative gain in entropy of bulk water, upon heating.[42] The near-native intermediate is thus regarded as a desolvated state relative to the native state. This trend is reversed above 65 °C, where the protein now exhibits an increased presence of water in the hydrophobic core. Because the eight individual solvent isotope changes possess a similar trend, this reentry of water likely represents a cooperative process.

To complement water accessibility through solvent isotope shifts, paramagnetic shifts from dissolved oxygen provide a perspective on the local density and hydrophobicity in the protein interior.[43] Oxygen can be readily introduced to the protein by equilibrating the sample at a partial pressure of 10–25 bar. O_2 then partitions into the hydrophobic core, establishing concentration gradients, where a local O_2 concentration can be ascertained on the basis of the magnitude of the paramagnetic shift. Generally, such shifts depend linearly on the local O_2 concentration below pressures of 50 bar.[44,45] We define a normalized quantity, $\Delta\delta^*(O_2)$, relative to the paramagnetic shift observed on the 4F-Phe standard. Figure 6a shows the normalized paramagnetic shifts, $\Delta\delta^*(O_2)$, resulting from the dissolved oxygen as a function of the temperature. Paramagnetic shifts exhibit a prominent increase with temperature, to the point where $\Delta\delta^*(O_2)$ is between 1 and 18 times that observed with the 4F-Phe standard at a temperature nearly coinciding with T_{NI} associated with the onset of the near-native intermediate. This is in sharp contrast to the expected norm for compact proteins, where the average oxygen concentration in the interior of the protein is known to be less than that in water,[46] whereas that in the interior of a micelle is an order of magnitude higher than that in water.[47] Oxygen accessibility is influenced by both hydrophobicity and local density. As temperature increases and protein fluctuations become more prevalent, local void volumes are created in the protein interior, which facilitates the solubilization of oxygen. This increased partitioning of oxygen to the protein interior with temperature is reversed above 65 °C, where oxygen solubility is seen to decrease and the interior becomes hydrated. A van't Hoff analysis of the temperature dependence of the partition coefficients of oxygen to the protein interior, $K_p = [O_2]_{in}/[O_2]_{out}$, between 25 and 65 °C reveals that the partitioning of oxygen to the hydrophobic core is strongly entropically driven (ΔS = 88.1 J K^{-1} mol^{-1}, as shown in Table S1 of the Supporting Information) and remarkably similar to that measured recently in micelles.[47] The results suggest that the environment of the protein interior is disordered and more liquid alkanelike near T_{NI} (i.e., highly dynamic and hydrophobic). Although it is well-known that hydrophobic forces play a greater role at higher temperatures, the significant role of entropy and the similarity from the perspective of access by O_2 is consistent with previous descriptions of hydrophobic forces in the protein interior.[9]

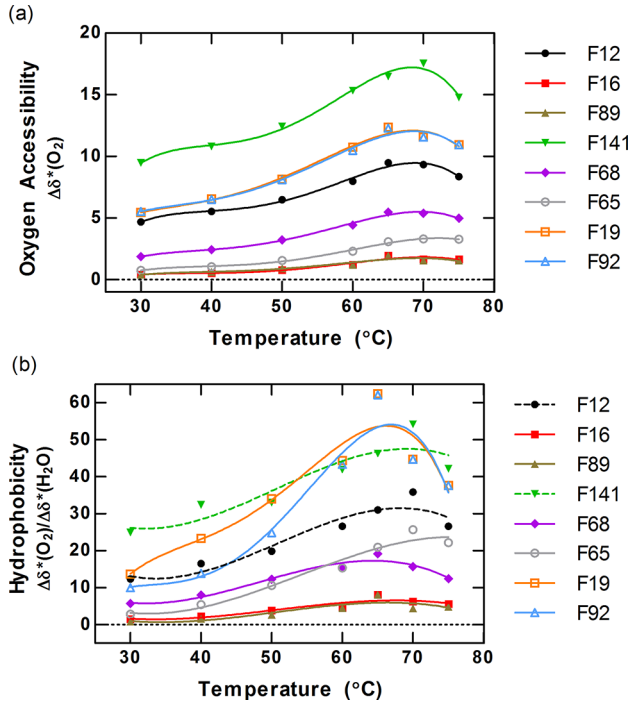

Figure 6. Temperature-dependent changes in oxygen accessibility and hydrophobicity. (a) Oxygen accessibility to the protein interior as measured by the temperature dependence of ^{19}F paramagnetic shifts, $\Delta\delta^*(O_2)$, resulting from the dissolution of oxygen under a partial pressure of 20 bar. Paramagnetic shifts are normalized by the paramagnetic shifts observed for an internal standard, 4F-Phe. (b) Hydrophobicity as measured by the relative partitioning of oxygen and water, which is described through a ratio of the normalized oxygen-induced paramagnetic shifts to normalized solvent isotope shifts. Note that the solvent isotope shifts of F12 and F141 have been renormalized to values representative of the average solvent exposure of the remaining six 3F-Phe residues ($\Delta\delta^*(H_2O)$ (30 °C) = 0.3).

The solvent isotope shifts and paramagnetic shifts, which measure local oxygen accessibility, may be combined in a quotient, $\Delta\delta^*(O_2)/\Delta\delta^*(H_2O)$, reflecting the local hydrophobicity. Most definitions of hydrophobicity incorporate a partition coefficient associated with the transfer of a molecule of interest from a polar to a nonpolar environment.[48] In our case, we make use of the different chemical potentials of water and O_2 to study the hydrophobicity of a point of interest in the protein interior. Effectively, we measure the ratio of the partition coefficients associated with H_2O and O_2 between water and the protein interior. Thus, we define a hydrophobicity parameter at a specific site, i, in terms of the respective ratio of concentrations of the probe species in the bulk water phase and the protein interior

$$\text{Hydrophobicity} = \frac{[O_2]_i/[O_2]_{bulk}}{[H_2O]_i/[H_2O]_{bulk}} \quad (1)$$

dx.doi.org/10.1021/bi4010057 | Biochemistry 2013, 52, 5780–5789

Assuming the oxygen paramagnetic shifts and solvent isotope shifts are proportional to the respective probe concentrations, the experimentally determined quotient, $\Delta\delta^*(O_2)/\Delta\delta^*(H_2O)$, will equal the above hydrophobicity quotient as long as the geometric considerations of the accessibility of water and O_2 are regarded as equal.[49−51] Figure 6b depicts the hydrophobicity quotient, $\Delta\delta^*(O_2)/\Delta\delta^*(H_2O)$, as a function of temperature. Hydrophobicity thus exhibits a maximum at the temperature associated with the transition to the folding intermediate, whereupon increased temperature results in a gradual unfolding and loss of hydrophobicity.

NMR Studies of the Compactness of the Native State and the Desolvated Near-Native Intermediate. The extent of compactness can be studied in greater detail by several NMR experiments: (1) nuclear Overhauser effect spectroscopy (NOESY) experiments focused on contacts between aromatic side chains and aliphatics, (2) spin diffusion from the aliphatic side chains to the protein backbone amides, (3) diffusion measurements that monitor the protein hydrodynamic radius, and (4) $^{13}C,^{1}H$ heteronuclear multiple quantum correlation (HMQC) experiments focused on the methyl groups located in the hydrophobic core of the protein. The $^{1}H,^{1}H$ NOESY spectra of 3F-Phe-enriched CaM reveal a marked decrease in the aromatic−aliphatic cross-peak intensity above 50 °C (Supporting Information, Figure S4). The decrease in inter-residue NOE contacts is qualitatively consistent with the notion of a more dynamic and less well-packed hydrophobic interior.[6] However, the NOE as presented is complicated by the known dependence of cross-relaxation on the temperature-dependent tumbling time as well as the simultaneous effects of both distance and angular averaging, which is discussed in detail elsewhere.[26,52,53] Clustering can also be visualized by spin-diffusion measurements in which the backbone amide signal is monitored while the aliphatic interior of the protein is selectively saturated.[54] The intensity of the majority of the amide ^{1}H signals, upon saturating the aliphatic region of the spectrum, generally decreases. With increased temperature, this effect is diminished, signifying that the aliphatic side-chain isomerizations within the hydrophobic core are becoming less restricted (Supporting Information, Figure S5). The gradual loss of rigidity of the hydrophobic core results in less efficient spin diffusion. This loss in rigidity is anticipated to result in a corresponding gain in the hydrodynamic radius of the protein. NMR-based diffusion measurements of CaM reveal an increase in the hydrodynamic radius with increasing temperature followed by a modest plateau near the temperature regime where the folding intermediate exists (Supporting Information, Figure S6). The natural abundance $^{13}C,^{1}H$ HMQC methyl spectra of 3F-Phe-enriched CaM corroborate the idea that the hydrophobic core is more dynamic, showing a clear convergence of methyl resonances with temperature (Supporting Information, Figure S7). At 37 °C, the methyl resonances, most of which arise from the hydrophobic core, are well resolved and exhibit a prominent dispersion. This dispersion is diminished at 65 °C, signifying a more dynamic hydrophobic interior. Taken together, these experiments suggest that the desolvated near-native intermediate adopts a more dynamic state with an expanded hydrophobic interior.

Folding Kinetics between the Near-Native Intermediate and the Folded State. Although the ^{19}F NMR solvent isotope shifts and paramagnetic shifts identify a folding intermediate and give some sense of the compactness and the role of water in this near-native state, we next consider experiments that identify the folding and unfolding rates, k_{NI} and k_{IN}, between the native and near-native states. In particular, CPMG relaxation dispersion experiments provide a measure of the chemical exchange processes by monitoring the transverse magnetization relaxation rates as a function of the separation between 180° refocusing pulses, τ_{cp}.[55,56] In the fast exchange limit, assuming the system can be approximated by two states, N and I, separated by a chemical shift, $\Delta\omega$, the exchange contribution to the transverse spin relaxation rate is given by[57]

$$R_{ex} = \frac{p_1 p_2 (\Delta\omega)^2}{k_{ex}}\left(1 - \frac{2}{k_{ex}\tau_{cp}}\tanh\frac{k_{ex}\tau_{cp}}{2}\right) \quad (2)$$

$$k_{ex} = \frac{k_{IN}}{p_1} = \frac{k_{NI}}{p_2}$$

$$0.5 \le p_1 \le 1$$

$$p_2 = (1 - p_1)$$

where k_{ex} is expressed in terms of the folding and unfolding rates and the fraction of each of the two states, p_1 and p_2. CPMG relaxation rate dispersion curves (i.e., $R_{2,eff}$ versus $^{1}/_{2}$ τ_{cp}) obtained from measurements at 57 °C (i.e., below the temperature associated with transition to the near-native state) suggest that CaM undergoes two-site exchange on a time scale of 2400 Hz (Figure 7). Although all residues exhibit dispersions, those of residues 19, 68, and 92 are the most pronounced. These dispersions can be detected between 45 and 57 °C (the highest available temperature on the cryogenic NMR probe). At the same time, CPMG relaxation dispersion measurements, on the basis of the ^{15}N transverse relaxation, reveal no millisecond time-scale dynamics, from which we conclude that the conformational exchange involves a subtle change that is associated primarily with the hydrophobic interior of the protein. Two results connect the observed fluctuations to the transition between the native and near-native states: (1) The addition of the cosolvent, trifluoroethanol (TFE), which is known to stabilize the folded state, completely removes the observed dispersion and (2) the dispersions can only be observed between 40 and 65 °C, coincident with the temperature regime in which the near native state is believed to be populated.

DISCUSSION

Role of the Near-Native Desolvated Intermediate in Folding and Misfolding. The classic notion of protein folding posits that the process is largely driven by hydrophobic collapse in which the release of waters of hydration from the unfolded polypeptide results in a net gain in entropy, thereby propelling the protein into a folded state. More recent descriptions emphasize the role of backbone hydrogen bonds in the early stages of folding.[58] In this case, the secondary structure and overall topology is expected to be established prior to hydrophobic collapse. Our data shows that an intermediate, consistent with a dry near-native state,[11,12,59,60] is established along the temperature-denaturation pathway. Upon heating from lower temperatures associated with the native state, the desolvation barriers decrease, reaching a point where water is released from the protein and the hydrophobic interior adopts a liquid alkanelike state. Moreover, the observed trends in the solvent isotope shifts, oxygen solubility, and hydrophobicity from 30 to 65 °C are consistent with theoretical

dx.doi.org/10.1021/bi4010057 | Biochemistry 2013, 52, 5780−5789

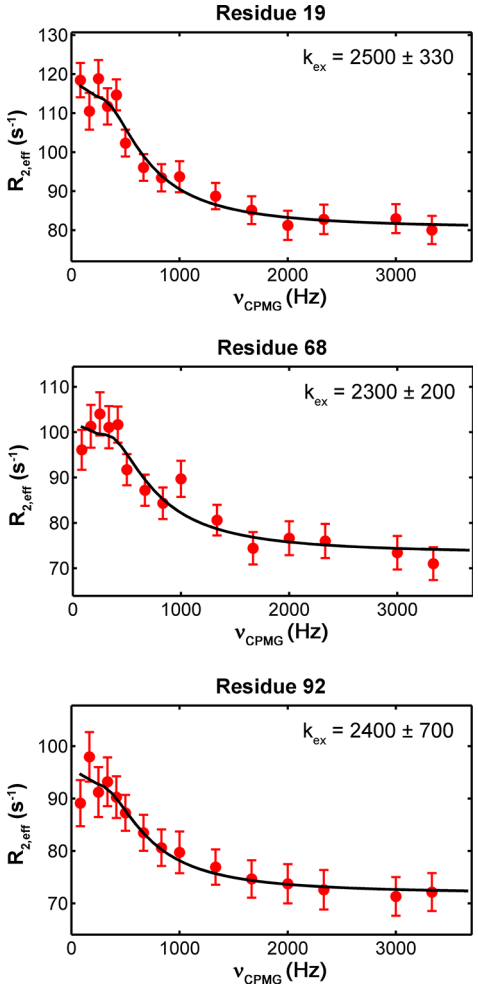

Figure 7. ^{19}F CPMG relaxation dispersion profiles for F68, F19, and F92 at 57 °C. Dispersion curves were fit to a two-state exchange model (eq 2) to obtain the exchange rate, k_{ex}, between state N and I.

descriptions that predict hydrophobic-interaction strengths to increase with temperature, as envisaged in Figure 8.[61,62] Others have also observed that hydrophobic forces, and in some instances (through changes in side-chain pK_a) internal salt linkages, tend to increase with higher temperatures.[63] The near-native intermediate state precedes protein compaction upon cooling and is characterized by a similar backbone structure to that of the native state and minimal solvent penetration. Moreover, the presence of greater dynamics within the hydrophobic interior provides a gain in configurational entropy, thereby stabilizing the intermediate. This would also represent an advantage in the folding process because diffusive searches toward the compact folded state would presumably be very fast. Others have noted the importance of configurational entropy in proteins such as calmodulin for the purposes of ligand binding while at the same time establishing the presence of conformers within the ensemble, which are consistent with the description of a dry molten globule.[64] The final step in the folding process is expected to be cooperative and facilitated by the closer association of the hydrophobic residues and the reentry of a few water molecules of hydration as the interior becomes close packed. Cheung and others have noted the importance of water in "lubricating" the protein-folding process.[65] Indeed, there are many examples in the literature in which folding intermediates are demonstrated to be hydrated, and a "wet" molten-globule state has been suggested. In our case, however, a dry near-native folding intermediate is clearly observed along the temperature-denaturation pathway, and there are potential consequences of such states to both function and to disease through protein aggregation and misfolding.

Calmodulin represents a ubiquitous and well-studied protein whose folding properties and dynamics have been the subject of intense study by scattering,[66] NMR,[14,15,67−70] and single-molecule force spectroscopy.[17,18,71,72] In particular, the recent single-molecule force spectroscopy experiments identified an elaborate ensemble of on- and off-pathway folding intermediates.[17] We note that the dry near-native state, which we observe at higher temperatures, may not be captured by single-molecule spectroscopy, although we do have evidence from CPMG measurements that this specific intermediate is populated at physiological temperatures (~40 °C). The challenge in observing this state by other means is that the conformational

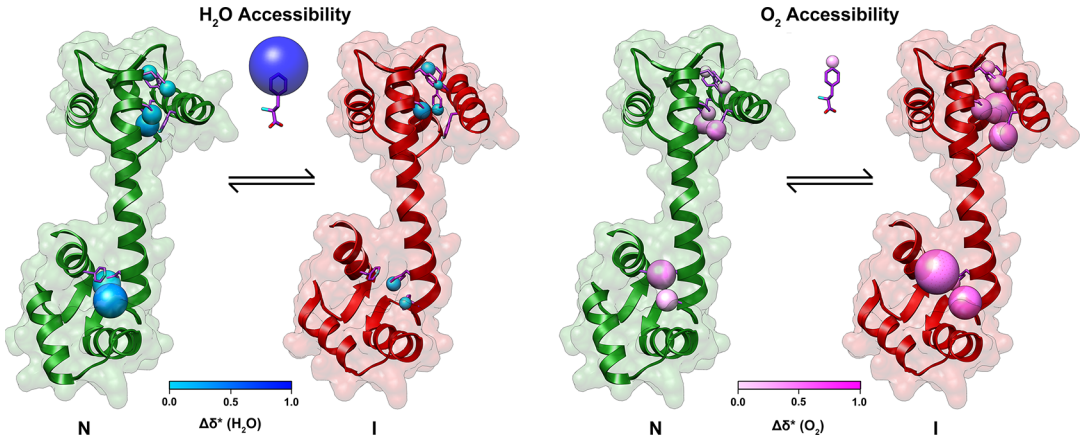

Figure 8. Graphical representation of water and oxygen accessibility in the native (N) and the near-native intermediate (I) states of CaM on the basis of the solvent isotope shifts ($\Delta\delta^*(H_2O)$) and paramagnetic shifts ($\Delta\delta^*(O_2)$) associated with 3F-Phe probes in the protein interior. Sites having a higher water or oxygen accessibility are shown with spheres having a larger radius and darker shade of blue or pink, respectively. Note that residues F12 and F141 exhibit solvent isotope shifts that are too small to be observed using the current scale. The depiction of the near-native intermediate structural model was constructed by slightly modifying the known native CaM structure to correspond to a slightly larger hydrodynamic radius.

dx.doi.org/10.1021/bi4010057 | *Biochemistry* 2013, 52, 5780−5789

changes appear to be quite subtle and the CPMG studies suggest that the state is also short-lived and in fast exchange with the native state.

CaM is somewhat atypical of globular proteins in that it is held together not only by hydrophobic forces but also by additional ionic forces via the four tightly bound calcium ions within the EF hands. Furthermore, the hydrophobic interior is recognized to be somewhat more dynamic than other globular proteins, which may explain the anomalously high degree of water and oxygen penetration observed in the vicinity of the phenylalanines in the protein interior, even for the native state.[68] As such, it is difficult to predict the extent to which such dry near-native intermediates may play a role in folding and misfolding in general. Another significant consideration is the potential loss of calcium at higher temperatures and the adoption of the apo state. The structure and $^{15}N,^{1}H$ NMR signature of the apo state are well-known from the literature and is easily distinguished from the calcium-loaded state.[38] Our $^{15}N,^{1}H$ NMR show no evidence of even a minor fraction of the apo state below 70 °C. At the same time, $^{15}N,^{1}H$ CPMG measurements show no evidence of even millisecond-lived apo conformers. Thus, the onset of a more hydrophobic state around 66 °C cannot be explained by the appearance of the apo conformation, whose interior is indeed expected to be more hydrophobic. Rather, we argue for an intact and desolvated near-native state of CaM.

In protein folding, desolvation may represent the rate-limiting step.[73] Upon establishing the dry near-native intermediate, the increased dynamics effectively provides greater sampling of the ensemble and a lowering of the barrier toward more fully folded conformers. The increased disorder inherent in the intermediate effectively accelerates the folding process, which involves the collapse of the (desolvated) hydrophobic core and stabilization of specific inter-residue contacts through van der Waals interactions, hydrogen bonds, and salt links. Although we do not imagine the folded state to be highly solvated, there are clearly specific waters of hydration involved in stabilizing the folded state, at least in the vicinity of the phenylalanines. These waters of hydration may also arise from higher-energy conformers that are more solvent exposed but associated with the native ensemble. The strength and density of the water interactions with the phenylalanine residues in the protein interior is diminished in the dry folding intermediate.[74] The main point is simply that the trajectory of solvent exposure along the temperature folding/unfolding pathway involves a desolvation step and the establishment of a dry near-native state whose hydrodynamic radius is increased.

The role of a dry near-native folding intermediate in misfolding is also intriguing. The rate-limiting step in protein aggregation is often desolvation. In studies of amyloidosis, protein aggregation and fibril formation is achieved once a partially unfolded metastable state is reached.[75] If the intermediate is more dynamic, then one might expect rare conformational excursions that lead irreversibly to misfolded states. In the case of a desolvated intermediate, distinct and likely transient states may be more predisposed to aggregation through non-native hydrophobic contacts. Although CaM is admittedly a model protein with no connection to amyloidosis, we have observed the formation of aggregated states upon incubation of CaM over periods of weeks at temperatures near the transition to the near-native state (~60 °C). Moreover, the incorporation of 5% TFE, which is known to stabilize the native state and prevent excursions to the near-native intermediate, results in no detectable aggregates under the same conditions (data not shown).

CONCLUSIONS

This study considers the topology of a well-known soluble protein, calmodulin, along the protein folding/unfolding pathway established by temperature. Although it is difficult to reversibly unfold CaM, it is possible to explore structural and dynamic properties of this protein up to a temperature of 70 °C. Around 66 °C, we detect a folding intermediate whose backbone structure is nativelike, as judged by CD and $^{15}N,^{1}H$ NMR spectroscopy. ^{19}F NMR solvent isotope shifts show that the water accessibility is clearly reduced in the hydrophobic interior upon attaining the folding intermediate, addressing a longstanding debate regarding the existence of dry near-native intermediates. The combination of solvent isotope shifts and O_2 paramagnetic shifts give a detailed microscopic perspective of both solvent exposure and hydrophobicity. Moreover, CPMG measurements point toward the existence of the near-native state at physiological temperatures, although we cannot say if such a state is on-pathway between the native and unfolded states at physiological temperatures. On the basis of the NMR observations of CaM as a function of temperature, we conclude that folding can occur by a rapid and early acquisition of secondary structure and hydrogen bonds until a "dry" near-native intermediate is attained. Given the high extent of disorder associated with this intermediate, it can then diffusively explore conformations that allow it to adopt a fully folded compact state. Taken together, it is clear that protein folding is far from a simple two-state cooperative process, at least in the case of CaM.

ASSOCIATED CONTENT

Supporting Information

Detailed information on the protein expression and purification, NMR experiments performed at two field strengths, and mathematical analyses for the estimated populations of the native and near-native states, solvent isotope experiments, O_2 paramagnetic shifts, hydrophobicity measurements, and CPMG relaxation dispersion measurements; far- and near-UV ellipticity as a function of temperature for CaM; fits of the imposed two-state model to the ^{19}F NMR chemical-shift data, NOESY spectra of 3F-Phe-enriched CaM; spin-diffusion measurements, hydrodynamic radius measurements of 70% 3F-Phe-enriched CaM; ^{13}C and ^{1}H HMQC methyl spectra of 70% 3F-Phe-enriched CaM; and enthalpies and entropies associated with the partitioning of oxygen in the vicinity of the eight 3F-Phe reporters. This material is available free of charge via the Internet at http://pubs.acs.org.

AUTHOR INFORMATION

Corresponding Author

*Tel: 905-828-3802; E-mail: scott.prosser@utoronto.ca.

Author Contributions

§These authors contributed equally.

Funding

This work was supported by an NSERC research discovery award (grant no. 261980) and by CIHR (CIHR Training Program in Protein Folding and Interaction Dynamics: Principles and Diseases).

Notes

The authors declare no competing financial interest.

■ ACKNOWLEDGMENTS

We are thankful to Voula Kanelis, John Rubinstein, Hue Sun Chan, Julie Forman-Kay, and Lewis Kay (University of Toronto) for their comments. We would also thank Professor Leo Spyracopoulos and Craig Markin (University of Alberta) for helpful discussions.

■ ABBREVIATIONS

3F-Phe, 3-fluorophenylalanine; CaM, calmodulin; CD, circular dichorism; HSQC, heteronuclear single quantum coherence; HMQC, heteronuclear multiple quantum coherence; NOESY, nuclear Overhauser effect spectroscopy; ROESY, rotating frame Overhauser effect spectroscopy

■ REFERENCES

(1) Kubelka, J., Hofrichter, J., and Eaton, W. A. (2004) The protein folding 'speed limit'. *Curr. Opin. Struct. Biol. 14*, 76−88.

(2) Udgaonkar, J. B., and Baldwin, R. L. (1988) NMR evidence for an early framework intermediate on the folding pathway of ribonuclease-A. *Nature 335*, 694−699.

(3) Itzhaki, L. S., Otzen, D. E., and Fersht, A. R. (1995) The structure of the transition-state for folding of chymotrypsin inhibitor-2 analyzed by protein engineering methods: Evidence for a nucleation-condensation mechanism for protein-folding. *J. Mol. Biol. 254*, 260−288.

(4) Teufel, D. P., Johnson, C. M., Lum, J. K., and Neuweiler, H. (2011) Backbone-driven collapse in unfolded protein chains. *J. Mol. Biol. 409*, 250−262.

(5) Dickinson, E., and Matsumura, Y. (1994) Proteins at liquid interfaces: Role of the molten globule state. *Colloids Surf., B 3*, 1−17.

(6) Arai, M., and Kuwajima, K. (2000) Role of the molten globule state in protein folding. *Adv. Protein Chem. 53*, 209−282.

(7) Armstrong, B. D., Choi, J., Lopez, C., Wesener, D. A., Hubbell, W., Cavagnero, S., and Han, S. (2011) Site-specific hydration dynamics in the nonpolar core of a molten globule by dynamic nuclear polarization of water. *J. Am. Chem. Soc. 133*, 5987−5995.

(8) Sosnick, T. R., and Barrick, D. (2011) The folding of single domain proteins − have we reached a consensus? *Curr. Opin. Struct. Biol. 21*, 12−24.

(9) Privalov, P. L., and Gill, S. J. (1988) Stability of protein-structure and hydrophobic interaction. *Adv. Protein Chem. 39*, 191−234.

(10) Feng, Y. Q., Sligar, S. G., and Wand, A. J. (1994) Solution structure of apocytochrome b562. *Nat. Struct. Biol. 1*, 30−35.

(11) Jha, S. K., and Udgaonkar, J. B. (2009) Direct evidence for a dry molten globule intermediate during the unfolding of a small protein. *Proc. Natl. Acad. Sci. U.S.A 106*, 12289−12294.

(12) Baldwin, R. L., Frieden, C., and Rose, G. D. (2010) Dry molten globule intermediates and the mechanism of protein unfolding. *Proteins: Struct., Funct., Bioinf. 78*, 2725−2737.

(13) Chattopadhyaya, R., Meador, W. E., Means, A. R., and Quiocho, F. A. (1992) Calmodulin structure refined at 1.7 Angstrom resolution. *J. Mol. Biol. 228*, 1177−1192.

(14) Lakowski, T. M., Lee, G. M., Okon, M., Reid, R. E., and Mcintosh, L. P. (2007) Calcium-induced folding of a fragment of calmodulin composed of EF-hands 2 and 3. *Protein Sci. 16*, 1119−1132.

(15) Anthis, N. J., Doucleff, M., and Clore, G. M. (2011) Transient, sparsely populated compact states of apo and calcium-loaded calmodulin probed by paramagnetic relaxation enhancement: Interplay of conformational selection and induced fit. *J. Am. Chem. Soc. 133*, 18966−18974.

(16) Shiba, K., Niidome, T., Katoh, E., Xiang, H., Han, L., Mori, T., and Katayama, Y. (2010) Polydispersity as a parameter for indicating the thermal stability of proteins by dynamic light scattering. *Anal. Sci. 26*, 659−663.

(17) Stigler, J., Ziegler, F., Gieseke, A., Gebhardt, J. C. M., and Rief, M. (2011) The complex folding network of single calmodulin molecules. *Science 334*, 512−516.

(18) Junker, J. P., and Rief, M. (2010) Evidence for a broad transition-states ensemble in calmodulin folding from single-molecule force spectroscopy. *Angew. Chem., Int. Ed. 49*, 3306−3309.

(19) Hull, W. E., and Sykes, B. D. (1975) Fluorotyrosine alkaline phosphatase. Internal mobility of individual tyrosines and role of chemical-shift anisotropy as a F-19 nuclear spin relaxation mechanism in proteins. *J. Mol. Biol. 98*, 121−153.

(20) Li, H. L., and Frieden, C. (2007) Observation of sequential steps in the folding of intestinal fatty acid binding protein using a slow folding mutant and F-19 NMR. *Proc. Natl. Acad. Sci. U.S.A 104*, 11993−11998.

(21) Lau, E., and Gerig, J. (2000) Origins of fluorine NMR chemical shifts in fluorine-containing proteins. *J. Am. Chem. Soc. 122*, 4408−4417.

(22) Otting, G. (1997) NMR studies of water bound to biological molecules. *Prog. Nucl. Magn. Reson. Spectrosc. 31*, 259−285.

(23) Modig, K., Liepinsh, E., Otting, G., and Halle, B. (2004) Dynamics of protein and peptide hydration. *J. Am. Chem. Soc. 126*, 102−114.

(24) Bruschweiler, R., and Wright, P. E. (1994) Water self-diffusion model for protein-water NMR cross-relaxation. *Chem. Phys. Lett. 229*, 75−81.

(25) Armstrong, B. D., and Han, S. G. (2009) Overhauser dynamic nuclear polarization to study local water dynamics. *J. Am. Chem. Soc. 131*, 4641−4647.

(26) Vogeli, B., Segawa, T. F., Leitz, D., Sobol, A., Choutko, A., Trzesniak, D., van Gunsteren, W., and Riek, R. (2009) Exact distances and internal dynamics of perdeuterated ubiquitin from NOE buildups. *J. Am. Chem. Soc. 131*, 17215−17225.

(27) Zhang, L. Y., Yang, Y., Kao, Y. T., Wang, L. J., and Zhong, D. P. (2009) Protein hydration dynamics and molecular mechanism of coupled water-protein fluctuations. *J. Am. Chem. Soc. 131*, 10677−10691.

(28) Nucci, N. V., Pometun, M. S., and Wand, A. J. (2011) Site-resolved measurement of water-protein interactions by solution NMR. *Nat. Struct. Mol. Biol. 18*, 245−250.

(29) King, J. T., Arthur, E. J., Brooks, C. L., and Kubarych, K. J. (2012) Site-specific hydration dynamics of globular proteins and the role of constrained water in solvent exchange with amphiphilic cosolvents. *J. Phys. Chem. B 116*, 5604−5611.

(30) Kitevski-LeBlanc, J. L., Evanics, F., and Prosser, R. S. (2010) Optimizing F-19 NMR protein spectroscopy by fractional biosynthetic labeling. *J. Biomol. NMR 48*, 113−121.

(31) Hoeltzli, S. D., and Frieden, C. (1995) Stopped-flow NMR spectroscopy: Real-time unfolding studies of 6-19F-tryptophan-labeled Escherichia coli dihydrofolate reductase. *Proc. Natl. Acad. Sci. U.S.A 92*, 9318−9322.

(32) Delaglio, F., Grzesiek, S., Vuister, G. W., Zhu, G., Pfeifer, J., and Bax, A. (1995) NMRPipe: A multidimensional spectral processing system based on unix pipes. *J. Biomol. NMR 6*, 277−293.

(33) Wagner, G., and Wuthrich, K. (1975) Proton NMR studies of aromatic residues in basic pancreatic trypsin inhibitor (BPTI). *J. Magn. Reson. 20*, 435−445.

(34) Baturin, S. J., Okon, M., and McIntosh, L. P. (2011) Structure, dynamics, and ionization equilibria of the tyrosine residues in Bacillus circulans xylanase. *J. Biomol. NMR 51*, 379−394.

(35) Skalicky, J. J., Mills, J. L., Sharma, S., and Szyperski, T. (2001) Aromatic ring-flipping in supercooled water: Implications for NMR-based structural biology of proteins. *J. Am. Chem. Soc. 123*, 388−397.

(36) Sykes, B. D., Weingarten, H. I., and Schlesinger, M. J. (1974) Fluorotyrosine alkaline phosphatase from Escherichia coli: Preparation, properties, and fluorine-19 nuclear magnetic resonance spectrum. *Proc. Natl. Acad. Sci. U.S.A 71*, 469−473.

(37) Kitevski-LeBlanc, J. L., Evanics, F., and Prosser, R. S. (2009) Approaches for the measurement of solvent exposure in proteins by F-19 NMR. *J. Biomol. NMR 45*, 255−264.

(38) Zhang, M., Tanaka, T., and Ikura, M. (1995) Calcium-induced conformational transition revealed by the solution structure of apo calmodulin. *Nat. Struct. Biol. 2*, 758−767.
(39) Stoclet, J. C., Gerard, D., Kilhoffer, M. C., Lugnier, C., Miller, R., and Schaeffer, P. (1987) Calmodulin and its role in intracellular calcium regulation. *Prog. Neurobiol. 29*, 321−364.
(40) Fraser, J. S., van den Bedem, H., Samelson, A. J., Lang, P. T., Holton, J. M., Echols, N., and Alber, T. (2011) Accessing protein conformational ensembles using room-temperature X-ray crystallography. *Proc. Natl. Acad. Sci. U.S.A 108*, 16247−16252.
(41) Wrabl, J. O., Gu, J. N., Liu, T., Schrank, T. P., Whitten, S. T., and Hilser, V. J. (2011) The role of protein conformational fluctuations in allostery, function, and evolution. *Biophys. Chem. 159*, 129−141.
(42) Shimizu, S., and Chan, H. (2000) Temperature dependence of hydrophobic interactions: a mean force perspective, effects of water density, and nonadditivity of thermodynamic signatures. *J. Chem. Phys. 113*, 4683.
(43) Teng, C.-L., and Bryant, R. G. (2004) Mapping oxygen accessibility to ribonuclease a using high-resolution NMR relaxation spectroscopy. *Biophys. J. 86*, 1713−1725.
(44) Prosser, R. S., and Luchette, P. A. (2004) An NMR study of the origin of dioxygen-induced spin-lattice relaxation enhancement and chemical shift perturbation. *J. Magn. Reson. 171*, 225−232.
(45) Prosser, R. S., Luchette, P. A., Westerman, P. W., Rozek, A., and Hancock, R. E. (2001) Determination of membrane immersion depth with O2: A high-pressure (19)F NMR study. *Biophys. J. 80*, 1406−1416.
(46) Hernandez, G., Teng, C. L., Bryant, R. G., and LeMaster, D. M. (2002) O2 penetration and proton burial depth in proteins: Applicability to fold family recognition. *J. Am. Chem. Soc. 124*, 4463−4472.
(47) Al-Abdul-Wahid, M. S., Evanics, F., and Prosser, R. S. (2011) Dioxygen transmembrane distributions and partitioning thermodynamics in lipid bilayers and micelles. *Biochemistry 50*, 3975−3983.
(48) Black, S. D., and Mould, D. R. (1991) Development of hydrophobicity parameters to analyze proteins which bear posttranslational or cotranslational modifications. *Anal. Biochem. 193*, 72−82.
(49) Evanics, F., Bezsonova, I., Marsh, J., Kitevski, J. L., Forman-Kay, J. D., and Prosser, R. S. (2006) Tryptophan solvent exposure in folded and unfolded states of an SH3 domain by 19F and 1H NMR. *Biochemistry 45*, 14120−14128.
(50) Bezsonova, I., Evanics, F., Marsh, J. A., Forman-Kay, J. D., and Prosser, R. S. (2007) Oxygen as a paramagnetic probe of clustering and solvent exposure in folded and unfolded states of an SH3 domain. *J. Am. Chem. Soc. 129*, 1826−1835.
(51) Evanics, F., Kitevski, J. L., Bezsonova, I., Forman Kay, J. D., and Prosser, R. S. (2007) 19F NMR studies of solvent exposure and peptide binding to an SH3 domain. *Biochim. Biophys. Acta 1770*, 221−230.
(52) Yip, P., and Case, D. A. (1989) A new method for refinement of macromolecular structures based on nuclear Overhauser effect spectra. *J. Magn. Reson. 83*, 643−648.
(53) Bruschweiler, R. (2003) New approaches to the dynamic interpretation and prediction of NMR relaxation data from proteins. *Curr. Opin. Struct. Biol. 13*, 175−183.
(54) Kutyshenko, V. P., and Cortijo, M. (2000) Water-protein interactions in the molten-globule state of carbonic anhydrase b: An NMR spin-diffusion study. *Protein Sci. 9*, 1540−1547.
(55) Palmer, A. G., Kroenke, C. D., and Loria, J. P. (2001) Nuclear magnetic resonance methods for quantifying microsecond-to-millisecond motions in biological macromolecules. *Methods Enzymol. 339*, 204−238.
(56) Baldwin, A., and Kay, L. (2009) NMR spectroscopy brings invisible protein states into focus. *Nat. Chem. Biol. 5*, 808−814.
(57) Luz, Z., and Meiboom, S. (1963) Nuclear magnetic resonance study of protolysis of trimethylammonium ion in aqueous solution − Order of the reaction with respect to solvent. *J. Chem. Phys. 39*, 366−371.
(58) Holthauzen, L. M. F., Rosgen, J., and Bolen, D. W. (2010) Hydrogen bonding progressively strengthens upon transfer of the protein urea-denatured state to water and protecting osmolytes. *Biochemistry 49*, 1310−1318.
(59) Finkelstein, A. V., and Shakhnovich, E. I. (1989) Theory of cooperative transitions in protein molecules. 2. Phase-diagram for a protein molecule in solution. *Biopolymers 28*, 1681−1694.
(60) Kiefhaber, T., Labhardt, A. M., and Baldwin, R. L. (1995) Direct NMR evidence for an intermediate preceding the rate-limiting step in the unfolding of ribonuclease-A. *Nature 375*, 513−515.
(61) Shimizu, S., and Chan, H. (2002) Origins of protein denatured state compactness and hydrophobic clustering in aqueous urea: inferences from nonpolar potentials of mean force. *Proteins: Struct., Funct., Bioinf. 49*, 560−566.
(62) Moghaddam, M., and Chan, H. (2007) Pressure and temperature dependence of hydrophobic hydration: Volumetric, compressibility, and thermodynamic signatures. *J. Chem. Phys. 126*, 114507-1−114507-15.
(63) Vinther, J. M., Kristensen, S. M., and Led, J. J. (2011) Enhanced stability of a protein with increasing temperature. *J. Am. Chem. Soc. 133*, 271−278.
(64) Fu, Y. N., Kasinath, V., Moorman, V. R., Nucci, N. V., Hilser, V. J., and Wand, A. J. (2012) Coupled motion in proteins revealed by pressure perturbation. *J. Am. Chem. Soc. 134*, 8543−8550.
(65) Cheung, M. S., García, A. E., and Onuchic, J. N. (2002) Protein folding mediated by solvation: Water expulsion and formation of the hydrophobic core occur after the structural collapse. *Proc. Natl. Acad. Sci. U.S.A 99*, 685−690.
(66) Yamada, Y., Matsuo, T., Iwamoto, H., and Yagi, N. (2012) A compact intermediate state of calmodulin in the process of target binding. *Biochemistry 51*, 3963−3970.
(67) Tjandra, N., Kuboniwa, H., Ren, H., and BAX, A. (1995) Rotational dynamics of calcium free calmodulin studied by 15N NMR relaxation measurements. *Eur. J. Biochem. 230*, 1014−1024.
(68) Lee, A. L., Kinnear, S. A., and Wand, A. J. (2000) Redistribution and loss of side chain entropy upon formation of a calmodulin-peptide complex. *Nat. Struct. Biol. 7*, 72−77.
(69) Shapiro, Y. E., Polimeno, A., Freed, J. H., and Meirovitch, E. (2011) Methyl dynamics of a Ca2+-calmodulin-peptide complex from NMR/SRLS. *J. Phys. Chem. B 115*, 354−365.
(70) Latham, M. P., and Kay, L. E. (2012) Is buffer a good proxy for a crowded cell-like environment? A comparative NMR study of calmodulin side-chain dynamics in buffer and E. coli lysate. *PLoS One 7*, e48226-1−e48226-13.
(71) Junker, J. P., Ziegler, F., and Rief, M. (2009) Ligand-dependent equilibrium fluctuations of single calmodulin molecules. *Science 323*, 633−637.
(72) Stigler, J., and Rief, M. (2012) Calcium-dependent folding of single calmodulin molecules. *Proc. Natl. Acad. Sci. U.S.A 109*, 17814−17819.
(73) Thirumalai, D., Reddy, G., and Straub, J. E. (2012) Role of water in protein aggregation and amyloid polymorphism. *Acc. Chem. Res. 45*, 83−92.
(74) Porter, D., and Vollrath, F. (2012) Water mobility, denaturation and the glass transition in proteins. *Biochim. Biophys. Acta 1824*, 785−791.
(75) Reddy, G., Straubb, J. E., and Thirumalai, D. (2009) Dynamics of locking of peptides onto growing amyloid fibrils. *Proc. Natl. Acad. Sci. U.S.A 106*, 11948−11953.